IEEE Access
Multidisciplinary | Rapid Review | Open Access Journal

Received November 27, 2019, accepted December 7, 2019, date of publication December 12, 2019,
date of current version December 23, 2019.

Digital Object Identifier 10.1109/ACCESS.2019.2959012

Multi-Objective Day-Ahead Scheduling of Power Market Integrated With Wind Power Producers Considering Heat and Electricity Trading and Demand Response Programs

CHUNYAN LI, (Member, IEEE), YIMING YAO, CHENYU ZHAO, AND XIN WANG
State Key Laboratory of Power Transmission Equipment and System Security and New Technology, Chongqing University, Chongqing 400044, China
Corresponding author: Chunyan Li (lcycqu@cqu.edu.cn)

ABSTRACT The large-scale penetration of renewable energy, such as wind power, brings a lot of economic and environmental benefits to the grid, and it also causes hidden dangers in the reliability and security of the power system due to its uncertainty. As an effective demand-side management method, demand response has unique advantages in smoothing wind power fluctuations and mitigating grid pressure. This paper proposes a new model for the demand response aggregator (DRA) that includes both combined heat and power systems (CHPS) and energy storage devices. DRA can interact with the Independent system operator (ISO) through combined heat and power (CHP) units, energy storage devices, and the heat buffer tank to benefit from the electricity market and the thermal market simultaneously. At the same time, wind power producers (WPP) are modeled to turn wind power that was initially passively consumed into active market participants. The problem is modeled using an improved weighted method, which aims to take the diverse objectives of multiple market participants into account. The proposed model is tested on the modified IEEE RTS-24 test system to analyze the optimal scheduling strategies of each participant in the power market.

INDEX TERMS Combined heat and power, demand response, electricity market, electricity storage, wind power producer.

NOMENCLATURE

Most of the symbols and notations used throughout this paper are defined below for quick reference. Others are defined following their first appearances, as needed.

A. ABBREVIATIONS & INDICES

ISO	Independent system operator
Genco	Generator company
WPP	Wind power producer
DRA	Demand response aggregator
DRPs	Demand response programs
CHP	Combined heat and power
CHPS	Combined heat and power system
FOR	Feasible operation region of the CHP unit
i	Index of Genco & CHP unit
j	Index of WPP
t	Index of time
k	Index of the boiler unit
ω	Index of scenario
n, m	Index of node

B. PARAMETERS

NG	Number of Gencos
NW	Number of wind power producers
N_{chp}	Number of CHP units
N_{b}	Number of boil units
T	Length of time
A_i, B_i, B_i	Cost function coefficients of generator i
TU_i/TD_i	Minimum up/down time of generator i
RU_i/RD_i	Ramp up/down rate of generator i
$c_{startupi}/c_{shutdowni}$	Startup/shutdown cost of generator i
$C_j^{capital}$	Capital cost of WPP j

The associate editor coordinating the review of this manuscript and approving it for publication was Wei Wei.

$C_j^{M\&O}$	Maintenance and operation costs of WPP j
$P_{j,wind}^{max}$	Maximum capacity of WPP j
d_t^0	Original load demand at time t
$d_t^{Contract}$	Contract for consumers participating in incentive-based DRP
λ_t^0	Original electricity price at time t
Inc^{max}/Pen^{max}	Maximum amount of unit incentive/Penalty
K_1, K_2	Dissatisfaction coefficients of consumers
θ	Participation coefficients of consumers integrated with DRPs
E	Price elasticity of demand
$P_{i,A}^{CHP}, P_{i,B}^{CHP}, P_{i,C}^{CHP}, P_{i,D}^{CHP}$	Electricity output of CHP unit i at four marginal points of the FOR
$H_{i,A}^{CHP}, H_{i,B}^{CHP}, H_{i,C}^{CHP}, H_{i,D}^{CHP}$	Heat output of CHP unit i at four marginal points of the FOR
M	An adequately large number
$a_i, b_i, c_i, d_i, e_i, f_i$	Cost function coefficients of the CHP unit
$\psi_{k,t}$	Cost function coefficients of the boiler unit
$H_k^{b,min}/H_k^{b,max}$	Minimum/maximum heat output of the boiler unit
R_i^{up}, R_i^{down}	Ramp up/down rate of CHP unit i
UT_i/DT_i	Minimum up/down time of CHP unit i
$\beta_{loss}/\beta_{gain}$	Heat generation loss/excess for the CHP unit during startup/shutdown period
B_{min}/B_{max}	Minimum/maximum heat buffer tank capacity
η	Heat loss rate for the heat buffer tank
$B_{max}^{charge}/B_{max}^{discharge}$	The maximum charge(discharge) rate of the heat buffer tank
H_t^D	Heat demand at time t
M^{char}/M^{dis}	Charge/discharge rate of the energy storage device
η^{char}/η^{dis}	Charging and discharging inefficiency of the energy storage device
S^{min}/S^{max}	Minimum/maximum capacity of the energy storage device
h_t	Thermal price at time t
τ_t	Unit income of heat buffer tank for selling heat to the ISO
$TB_{n,m}$	Susceptance of transmission line connecting buses n and m
$PF_{n,m}$	Capacity of transmission line connecting buses n and m

C. DECISION VARIABLES

$P_{gencoi,t}$	Scheduled output of Genco i at time t
λ_t	Electricity price at time
$x_{i,t}$	Binary variable for commitment status of generator i at time t
$y_{i,t}$	Binary variable for startup status of generator i at time t
$z_{i,t}$	Binary variable for shutdown status of generator i at time t
$P_{windj,t}$	Scheduled output of WPP j at time t
$\Delta_{j,t,\omega}$	Total deviations of wind power
$\Delta_{j,t,\omega}^+/\Delta_{j,t,\omega}^-$	Positive/negative deviations of wind power
$\sigma_{j,t}^+/\sigma_{j,t}^-$	unit income for positive/negative deviations of wind power
$P_{j,t,\omega wind}$	Output of WPP j at time t in scenario ω
d_t	Load demand at time t after implementing DRPs
Δd_t	Load change at time t after implementing DRPs
Inc_t	Incentive to the customer at time t for each MWh load reduction
γ_t	The total incentive for taking part in incentive-based DRP at time t
Pen_t	Penalty of the customer at time t for each MWh load reduction deviated from the contract level
μ_t	The total penalty for taking part in incentive-based DRP at time t
C	Dissatisfaction cost function of consumers
$P_{i,t}^{CHP}$	Produced power from CHP unit i at time t
$H_{i,t}^{CHP}$	Produced heat from CHP unit i at time t
$V_{i,t}$	Binary variable for commitment status of CHP unit i at time t
$V_{k,t}$	Binary variable for commitment status of boiler unit k at time t
$H_{k,t}^b$	Produced heat from boiler unit k at time t
$SU_{i,t}$	Binary variable for startup status of CHP unit i at time t
$SD_{i,t}$	Binary variable for shutdown status of CHP unit i at time t
$SU_{k,t}$	Binary variable for startup status of boiler unit k at time t
$SD_{k,t}$	Binary variable for shutdown status of boiler unit k at time t
zc_t	Charge amount of the energy storage device
zd_t	Discharge amount of energy storage device at time t
zd_{tsch}	the part of the electricity stored in the energy storage device for the load
s_t	Available electricity in the energy storage device at time t
σ_t	unit income of CHP unit for selling electricity to the ISO
Utility_t	Utility function of DRA at time t
$\theta_{n,t}$	Hour-t phase angle of node n

I. INTRODUCTION

Renewable energy, such as wind power and solar energy are environmentally friendly and economically convenient.

Therefore, countries around the world are vigorously promoting the construction of renewable energy power plants. The European Union, the United States, and China have respectively set the goal of achieving 100%, 80%, and 60% of renewable energy generation by 2050.

Although renewable energy generation has significant advantages, it also has deficiencies such as volatility and uncertainty, which will impact the reliability and security of power systems. The rational use of load-side resources such as demand response can help alleviate a series of problems brought about by the large-scale penetration of renewable energy.

Demand response program (DRP) according to the U.S. Department of Energy (DOE) is described as residential, industrial and commercial customers' proficiency to change energy-consumption schemes as a reaction to changes in the electricity price over time, or to incentive fees in order to fulfill reasonable prices and system reliability [1].

DRPs under this definition can be categorized into two groups: time-based and incentive-based. Time-based DRPs include Time of use (TOU), Real-time price (RTP), and Critical peak price (CPP). Incentive-based DRPs include programs such as Direct load control (DLC), Emergency demand response program (EDRP), and Interruptible/ curtailable (I/C) service.

Massively dispersed loads have made power dispatch more difficult. To integrate and utilize load-side resources, demand response aggregators (DRA) have emerged. As a link between customers and power markets, DRAs have a critical role in integrating and dispatching demand-side resources and participating in power markets. Researches on optimal operating strategies of DRAs to seek maximum profit while maintaining reliable and secure operation of the power system have attracted much attention.

Day-ahead energy schedule models of DRAs have been proposed in [2], [3], therein [2] models the detailed procedure of load shifting and curtailing, and [3] takes the financial risk caused by several uncertainties into account using the Conditional Value-at-Risk (CVaR) measure. However, both [2] and [3] have not considered the increment of consumers' dissatisfaction caused by load curtailment. In [4], [5], strategies of DRAs simultaneously participating in day-ahead and real-time markets have been analyzed. Reference [4] takes the uncertainty of electricity price into account through stochastic programming and [5] applies the information-gap decision theory (IGDT) in the self-scheduling problem to consider the uncertainties of electricity price and users' behaviors, which avoids computational burdens caused by stochastic programming approaches in [4].

The development of energy storage technology has promoted the popularization of storage devices on the demand side. Reference [6] proposes a game-theoretic structure between customers equipped with energy storage devices. Competition between DRAs to sell aggregated energy stored in storage devices directly to other aggregators in a market is modeled in [7]. Reference [8] proposes a networked Stackelberg competition, according to [7]. Although the energy storage devices in [6]–[8] can discharge electricity to the load, they do not consider the interactions between the energy storage device and the power system.

As the fastest-developing renewable energy in recent years, wind power installed capacity has proliferated, and researches on high wind power penetration earn a lot of attention [9]–[11]. Reference [12] emphasizes the importance of wind power producer (WPP) participating in the electricity market. [13] has analyzed the optimal offering strategies of WPPs in electricity markets. Optimal coordination of wind and thermal power has been addressed in several reports, such as [14]. Reference [15] focuses on optimal bidding strategy for pairing of wind and demand response resources. However, WPP plays the role of passive producers in [13], [14], which means that wind power is considered as energy to be consumed instead of an active market participant to make sure of the balance between supply and demand. In [15], there is no difference between WPP and traditional generators in clearing the market. WPP can also use demand response resources to decrease economic losses triggered by wind power fluctuations in [15].

Combined heat and power systems (CHPS) can produce electricity and heat simultaneously, which is economical and environmentally friendly. The efficiency of the combined heat and power (CHP) unit can achieve 70-85%, and it is becoming a hot spot in the current research. The CHP units can be categorized into six major technologies: fuel cells, micro-turbines, small steam turbines, sterling engines, reciprocating engines and small gas turbines [16]. The heat and electricity output of CHP units are non-separable and depend on each other with the constraint of the feasible operation region (FOR). The economic dispatch of the CHP unit is addressed in [17]. The schedule of electricity market considering demand response resources and CHPS is addressed in [18]–[22]. However, [18]–[21] do not model detailed DRPs, and [22] only takes time-based DRPs into account and uses a simple linear function to depict the relation between demand and electricity price. Reference [23] considers interconnected power distribution network and district heating network infrastructures through CHP units and heat pumps. The pricing method of heat and electricity is discussed in [24], [25].

To the best of our knowledge, there is no study of modeling DRA considering CHPS and energy storage devices simultaneously. CHPS and energy storage devices have developed rapidly in recent years, and they have become more and more widespread in the demand side. They can not only reduce generation costs, enhance power supply reliability and stability, but also increase the impact of the demand side in the power market.

Modeling DRA considering CHPS and energy storage device at the same time has many advantages. It can increase the flexibility of the demand side participating in the electricity market as well as enable DRAs to participate in the thermal market and earn profit.

This paper establishes a day-ahead power market framework with multiple market participants, including traditional generator company (Genco), WPP, and DRA with CHPS and energy storage devices. These market participants have different objective functions, that is, to maximize their profit. As the supreme leader in the power market, the Independent system operator (ISO) must take each part's interest into account when clearing the market to achieve the maximum of overall benefit. Therefore, it is necessary to establish a multi-objective optimization model based on each market participant's profit function and obtain the optimal strategy of each market participant under the premise of maximizing the overall benefit.

In summary, the main contributions of this paper are as follows:

a Modeling DRA considering CHPS and energy storage devices simultaneously; thus, DRA can participate in both the electricity market and the thermal market.
b Establishing a multi-objective day-ahead power market framework with multiple market participants, including Gencos, WPP, and DRA. WPP plays the role of active market participant, and there is no difference between WPP and traditional generators in clearing the market.
c Proposing an improved weighted method to solve the multi-objective optimization problem. The improved weighted method combines the Analytic Hierarchy Process and Entropy method to make the weighted coefficients more comprehensive.

In the remainder of this paper, Section II presents the model used in this work. The case studies are detailed in Section III. The paper is concluded in Section IV.

II. FORMULATION

A. TRADITIONAL GENCOS

Traditional Gencos rely mainly on coal-fired units for power generation. Although they will cause serious environmental pollution, it is still necessary to rely on traditional Gencos to maintain the stability and reliability of the power system in the current stage. The objective of Genco is formulated as (1):

$$\max(\text{Genco profit}) = \max(\sum_{i=1}^{NG}\sum_{t=1}^{T} P_{gencoi,t} * \lambda_t - C_{gencosti,t}) \quad (1)$$

The first term in (1) denotes the income obtained from participating in the day-ahead electricity market. The second term represents the operation cost of generators. The operation cost function of generator i at time t is formulated as (2):

$$C_{gencosti,t} = A_i * \left(P_{gencoi,t}\right)^2 + B_i * \left(P_{gencoi,t}\right) + C_i * x_{i,t} + C_{startupi,t} + C_{shutdowni,t} \quad (2)$$

The objective function should be maximized, considering the following constraints:

$$x_{i,t} - x_{i,t-1} = y_{i,t} - z_{i,t} \quad (3)$$
$$y_{i,t} + z_{i,t} \le 1 \quad (4)$$
$$y_{i,t} + \sum_{l=1}^{TU_i-1} z_{i,t+l} \le 1 \quad (5)$$
$$z_{i,t} + \sum_{l=1}^{TD_i-1} y_{i,t+l} \le 1 \quad (6)$$
$$x_{i,t} \cdot x_{i,t-1} \cdot \left(P_{gencoi,t} - P_{gencoi,t-1}\right) \le RU_i \quad (7)$$
$$x_{i,t} \cdot x_{i,t-1} \cdot \left(P_{gencoi,t-1} - P_{gencoi,t}\right) \le RD_i \quad (8)$$
$$P_i^{min} \cdot x_{i,t} \le P_{gencoi,t} \le P_i^{max} \cdot x_{i,t} \quad (9)$$
$$C_{startupi,t} = c_{startupi} * y_{i,t} \quad (10)$$
$$C_{shutdowni,t} = c_{shutdowni} * z_{i,t} \quad (11)$$

Constraints (3) and (4) impose restrictions on the generator's commitment status, startup status, and shutdown status. Constraints of minimum up and down times are expressed in (5) and (6). Constraints of ramp-up/down rate are denoted in (7) and (8). (9) represents the output limits of generators and (10)-(11) indicate the constraints of startup and shutdown cost.

B. WPP

In the model of this paper, WPP plays the role of an active participant in the electricity market, and there is no difference between WPP and traditional generators in clearing the market. Due to the uncertainty of wind power, the available wind power output may deviate from the planned output. If the actual output of wind power is less than the planned output, WPP will face a penalty; if the actual output of wind power is greater than the planned output, WPP can sell the excess wind power to ISO for profit. The objective of WPP is formulated as (12).

$$\begin{aligned}&\max(\text{WPP Profit})\\ &= \max(\sum_{j=1}^{NW}\sum_{t=1}^{T} P_{windj,t} * \lambda_t \\ &\quad + \mathrm{E}\left(\sigma_{j,t}^{+} * \Delta_{j,t,\omega}^{+} - \sigma_{j,t}^{-} * \Delta_{j,t,\omega}^{-}\right) - C_j^{capital} \\ &\quad - C_j^{M\&O} * P_{windj,t})\end{aligned} \quad (12)$$

The first term in (12) represents the income obtained from submitting the wind power output plan to the ISO. The second term denotes the expectation of income earned from the wind power deviations. The last two terms express maintenance and operation costs.

Constraints are as follows [27]:

$$0 \le P_{windj,t} \le P_{j,wind}^{max} \quad (13)$$
$$\Delta_{j,t,\omega} = P_{j,t,\omega wind} - P_{windj,t} \quad (14)$$
$$\Delta_{j,t,\omega} = \Delta_{j,t,\omega}^{+} - \Delta_{j,t,\omega}^{-} \quad (15)$$
$$0 \le \Delta_{j,t,\omega}^{+} \le P_{j,t,\omega wind} \quad (16)$$
$$0 \le \Delta_{j,t,\omega}^{-} \le P_{j,wind}^{max} \quad (17)$$

Constraints (13) impose restrictions on wind power output. Constraints of positive and negative wind power deviations are represented in (14-17). The maximum positive deviation occurs when the wind power output plan is zero, and the actual wind power output is not zero; the maximum negative

deviation occurs when the wind power output is scheduled at the maximum installed capacity, but the actual wind power output is zero.

C. DEMAND RESPONSE AGGREGATOR (DRA)

As a bridge between consumers and ISO, DRA plays a vitally important role in the rational planning of load curves and the consumption of renewable energy. This paper assumes that a fraction of consumers own CHPS and energy storage devices. CHPS includes the CHP unit, boiler unit, and heat buffer tank. With the rapid development of the smart grid, CHPS and storage devices will be more and more popular in the demand side.

1) MODELING OF DEMAND RESPONSE PROGRAMS

DRPs can be divided into time-based and incentive-based programs. This paper considers load participating in TOU and I/C programs at the same time.

The modeling process of incentive-based programs is shown first. Suppose that the customer changes his demand from d_t^0 (initial value) to d_t after implementing the load curtailing. The amount of load change is expressed in (18):

$$\Delta d_t = d_t - d_t^0 \tag{18}$$

ISO will provide incentives for DRAs participating in load curtailment:

$$\gamma_t = Inc_t \left(d_t^0 - d_t\right) \quad \forall t \in \mathrm{T} \tag{19}$$

Before the market-clearing, ISO will sign a contract with the DRA on the amount of load reduction. If the amount of load reduction does not meet the contract requirement, the DRA will be faced with a penalty. The total penalty at time t is denoted in (20):

$$\mu_t = Pen_t \left(d_t^{Contract} - \left(d_t^0 - d_t\right)\right) \quad \forall t \in \mathrm{T} \tag{20}$$

It is to be noted that both Inc_t and Pen_t in (19) and (20) are decision variables, and they must be constrained to (21) and (22).

$$0 \le Inc_t \le Inc^{max} \tag{21}$$

$$0 \le Pen_t \le Pen^{max} \tag{22}$$

The reduction of the load will affect the living quality of consumers, increasing consumer dissatisfaction. Equation (23) establishes an expression for consumer's dissatisfaction function [28]:

$$\mathrm{c} = K_1 \Delta {d_t}^2 + K_2 \Delta d_t - K_2 \Delta d_t \theta \tag{23}$$

K_1 and K_2 are dissatisfaction coefficients. θ is the customer type and is used to depict the enthusiasm of consumers to participate in DRPs. θ is normalized in the interval $0 \le \theta \le 1$, thus $\theta = 1$ for the most willing consumer and $\theta = 0$ for the least willing.

As for the time-based DRP, this paper uses the concept of price elasticity in economics to obtain the relationship between load and change in the electricity price.

Price elasticity, that is, the elasticity of demand to price, refers to the sensitivity of the corresponding change in the demand for a product when the price of a product changes, as shown in equation (24).

$$E = \frac{\lambda^0}{d^0} \cdot \frac{\partial d}{\partial \lambda} \tag{24}$$

The price elasticity of i time compared to j time can be derived from equation (24), as shown in (25):

$$E\,(i,j) = \frac{\lambda_j^0}{d_i^0} \cdot \frac{\partial d\,(i)}{\partial \lambda\,(j)} \tag{25}$$

Price elasticity can be divided into self-price elasticity and cross-price elasticity. The self-price elasticity coefficient is usually a negative value, and the cross-price elasticity coefficient is often a positive value, as shown in (26):

$$\begin{cases} E\,(i,j) \leqslant 0 & \text{if } i = j \\ E\,(i,j) \geqslant 0 & \text{if } i \neq j \end{cases} \tag{26}$$

The model of load fluctuating with the change of the electricity price, incentive and penalty is derived in [29], as can be seen in (27):

$$d_t = d_t^0 \cdot \{1 + E(t,t) \cdot \left[\frac{\lambda_t - \lambda_t^0}{\lambda_t^0} + \frac{\mathrm{Inc}_t + Pen_t}{\lambda_t^0}\right] + \sum_{\substack{j=1 \\ j \neq i}}^{24} E\,(t,j) \cdot \frac{\left[\lambda_j - \lambda_j^0 + \mathrm{Inc}_j + Pen_j\right]}{\lambda_j^0}\} \tag{27}$$

2) MODELING OF CHPS

CHPS includes CHP units, boiler units, and the heat buffer tank. There are two types of FOR for the CHP unit, as shown in Fig.1 and Fig.2 separately.

From Fig.1, it can be seen that the FOR is enclosed by the boundary curve ABCD, and it is constrained by three operational factors: maximum fuel consumption, minimum fuel consumption, and maximum heat extraction. The minimum and maximum fuel consumption is set at the amount that meets the 40-50% and 115% of rated power under normal conditions, respectively.

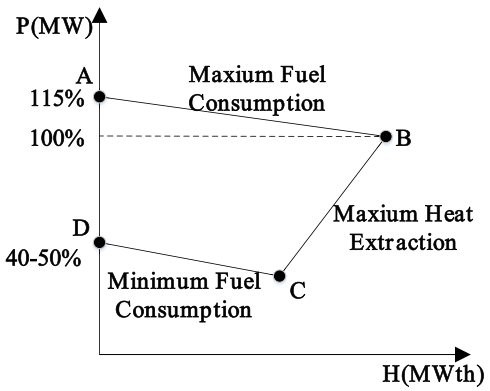

FIGURE 1. Power-heat feasible region for a CHP unit type 1.

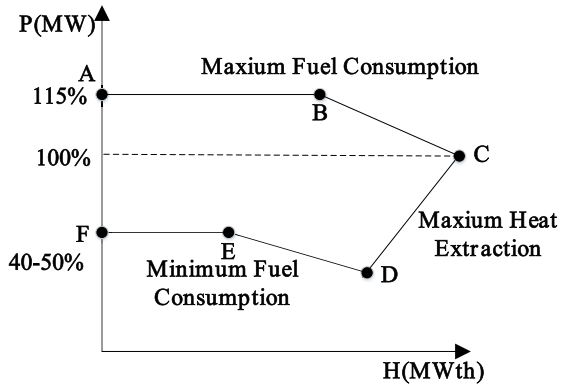

FIGURE 2. Power-heat feasible region for a CHP unit type 2.

The FOR of the type 2 CHP unit shown in Fig.2 is surrounded by the polygon ABCDEF, which is a non-convex feasible domain. For the sake of simplicity, only the FOR shown in Fig.1 is considered. In fact, for the non-convex FOR shown in Fig.2, it can be processed by the method of [17]. The main idea of this method is to solve the problem by splitting the non-convex feasible domain into two convex sub-regions by introducing integer auxiliary variables.

Equations (28-32) model the FOR of the type 1 CHP unit, as shown in Fig.1 [21]:

$$P_{i,t}^{\mathrm{CHP}} - P_{i,\mathrm{A}}^{\mathrm{CHP}} - \frac{P_{i,\mathrm{A}}^{\mathrm{CHP}} - P_{i,\mathrm{B}}^{\mathrm{CHP}}}{H_{i,\mathrm{A}}^{\mathrm{CHP}} - H_{i,\mathrm{B}}^{\mathrm{CHP}}} \left(H_{i,t}^{\mathrm{CHP}} - H_{i,A}^{\mathrm{CHP}}\right) \leq 0 \tag{28}$$

$$P_{i,t}^{\mathrm{CHP}} - P_{i,\mathrm{B}}^{\mathrm{CHP}} - \frac{P_{i,\mathrm{B}}^{\mathrm{CHP}} - P_{i,\mathrm{C}}^{\mathrm{CHP}}}{H_{i,\mathrm{B}}^{\mathrm{CHP}} - H_{i,\mathrm{C}}^{\mathrm{CHP}}} \left(H_{i,t}^{\mathrm{CHP}} - H_{i,\mathrm{B}}^{\mathrm{CHP}}\right) \geq -\left(1 - V_{i,t}\right) \times M \tag{29}$$

$$P_{i,t}^{\mathrm{CHP}} - P_{i,\mathrm{C}}^{\mathrm{CHP}} - \frac{P_{i,\mathrm{C}}^{\mathrm{CHP}} - P_{i,\mathrm{D}}^{\mathrm{CHP}}}{H_{i,\mathrm{C}}^{\mathrm{CHP}} - H_{i,\mathrm{D}}^{\mathrm{CHP}}} \left(H_{i,t}^{\mathrm{CHP}} - H_{i,\mathrm{C}}^{\mathrm{CHP}}\right) \geq -\left(1 - V_{i,t}\right) \times M \tag{30}$$

$$0 \leq H_{i,t}^{\mathrm{CHP}} \leq H_{i,\mathrm{B}}^{\mathrm{CHP}} \times V_{i,t} \tag{31}$$

$$0 \leq P_{i,t}^{\mathrm{CHP}} \leq P_{i,\mathrm{A}}^{\mathrm{CHP}} \times V_{i,t} \tag{32}$$

$$\forall i \in N_{chp}, \quad t \in T$$

In which, M is an adequately large number, and indices A, B, C, and D represent four vertices of the FOR.

The operating cost of the CHP unit i at hour t is shown in (33).

$$C_{i,t}^{CHP} = a_i \times P_{i,t}^{\mathrm{CHP}^2} + b_i \times P_{i,t}^{\mathrm{CHP}} + c_i + d_i \times H_{i,t}^{\mathrm{CHP}^2} + e_i \times H_{i,t}^{\mathrm{CHP}} + f_i \times H_{i,t}^{\mathrm{CHP}} \times P_{i,t}^{\mathrm{CHP}} \tag{33}$$

Equation (34) denotes the operating cost of the boiler unit k at hour t:

$$C_{k,t}^{\mathrm{B}} = \psi_{k,t} \times H_{k,t}^{\mathrm{b}} \tag{34}$$

In which, $H_{k,t}^{\mathrm{b}}$ refers to the produced heat from boiler unit k at time t and $\psi_{k,t}$ is the cost function coefficient of the boiler unit.

CHP units and boiler units should obey the constraints as follows:

$$\mathrm{SU}_{h,t} = V_{h,t} \times \left(1 - V_{h,t-1}\right), \quad h \in i,k \tag{35}$$

$$\mathrm{SD}_{h,t} = \left(1 - V_{h,t}\right) \times V_{h,t-1}, \quad h \in i,k \tag{36}$$

$$P_{h,t+1}^{CHP} - P_{h,t}^{CHP} \leq R_i^{\mathrm{up}}, \quad h \in i \tag{37}$$

$$P_{h,t}^{CHP} - P_{h,t+1}^{CHP} \leq R_i^{\mathrm{down}}, \quad h \in i \tag{38}$$

$$H_k^{\mathrm{b},min} \times V_{k,t} \leq H_{k,t}^{\mathrm{b}} \leq H_k^{\mathrm{b},max} \times V_{k,t} \tag{39}$$

$$SU_{h,t} + \sum_{l=1}^{UT_h - 1} SD_{\mathrm{h},t+l} \leq 1, \quad h \in i \tag{40}$$

$$SD_{h,t} + \sum_{l=1}^{DT_h - 1} SU_{h,t+l} \leq 1, \quad h \in i \tag{41}$$

Constraints (35) and (36) impose restrictions on the startup status and shutdown status of CHP units and boiler units. Constraints of ramp-up/down rate are denoted in (37) and (38). (39) represents the heat output limits of boiler units. Constraints of minimum up and down times are expressed in (40) and (41).

The heat generated by the CHP unit and the boiler unit is absorbed by the heat buffer tank. The total heat generated by the CHP unit and the boiler unit is as shown in (42):

$$\overline{H}_t = \sum_{i=1}^{N_{\mathrm{CHP}}} H_{i,t}^{\mathrm{CHP}} + \sum_{k=1}^{N_{\mathrm{b}}} H_{k,t}^{\mathrm{b}} \tag{42}$$

Considering the heat loss β_{loss} and gain β_{gain} during startup and shutdown periods, the heat actually absorbed by the heat buffer tank is as shown in (43):

$$H_t = \overline{H}_t - \beta_{\mathrm{loss}} SU_{h,t} + \beta_{\mathrm{gain}} SD_{h,t}, \quad h \in i,k \tag{43}$$

Hence, the available heat in the heat buffer tank, B_t, considering the heat loss rate η, could be calculated as:

$$B_t = (1 - \eta)\, B_{t-1} + H_t - H_t^D \tag{44}$$

The capacity constraints and ramp up/down rate constraints of the heat buffer tank are as shown in (45)-(47).

$$B_{min} \leq B_t \leq B_{max} \tag{45}$$

$$B_t - B_{t-1} \leq B_{max}^{\mathrm{charge}} \tag{46}$$

$$B_{t-1} - B_t \leq B_{max}^{\mathrm{discharge}} \tag{47}$$

3) MODELING OF ENERGY STORAGE DEVICES

This paper considers the interaction of energy storage devices with ISO. The energy storage device can not only purchase and store the electricity during the valley or off-peak period but also supply power to the load or sell electricity to ISO during the peak period of the electricity price. Its operational constraints are shown in (48)-(50):

$$zc_t \leq min\left\{M^{char}, S^{max} - s_t\right\} \quad \forall t \in T \tag{48}$$

$$zd_t \leq min\left\{M^{dis}, s_t\right\} \quad \forall t \in T \tag{49}$$

$$s_{t+1} - s_t - \eta^{char} zc_t + \frac{1}{\eta^{dis}} zd_t = 0 \quad \forall t \in T \tag{50}$$

4) OBJECTIVE FUNCTION OF DRA

After the implement of DRPs, the load can be partially powered by the CHPS and the energy storage device. The CHPS and energy storage device can sell excess electricity to ISO.

In addition to the electricity demand, the consumers studied in this paper have heat demand. The CHPS can supply heat to the consumers, and sell excess heat to ISO for profit.

Therefore, the DRA can interact with ISO through the CHPS and the energy storage device, that is, the DRA can participate in the electricity market as well as participate in the thermal market. The objective function of the DRA is as shown in (51).

$$\begin{aligned}\max(\text{DRA profit}) = \max \sum_{t=1}^{T} \{&(\text{Utility}_t + \gamma_t - \mu_t - c_t - \lambda_t \\ &* \left(d_t - P_{i,t,sch}^{\text{CHP}} - zd_{tsch}\right) - h_t \\ &* \left(H_t^D - H_{tsch}\right) + H_{tsell} * \tau_t) \\ &+ \sum_{i=1}^{NCHP} \left(P_{i,t}^{\text{CHP}} - P_{i,t,sch}^{\text{CHP}} - P_{i,t,chu}^{CHP}\right) * \sigma_t \\ &+ \sum_{i=1}^{NS} (zd_t - zd_{tsch}) * \sigma_t - zc_t * \lambda_t)\}\end{aligned} \tag{51}$$

In which, Utility_t is the utility function of consumers at time t, that is, the value that can be created by consuming the corresponding load. For commercial load, this value is equal to the commodity revenue that can be generated by consuming the corresponding load. In this paper, it is assumed that the utility function and the consumed load satisfy the quadratic function relationship, as shown in (52).

$$\text{Utility}_t = d_t^2 + d_t \tag{52}$$

$P_{i,t,sch}^{\text{CHP}}$ denotes the part of the electricity generated by the CHP unit for the load. $P_{i,t,chu}^{\text{CHP}}$ denotes the part of the electricity generated by the CHP unit for the energy storage device. H_{tsch} represents the part of the heat stored in the heat buffer tank for the load. H_{tsell} represents the part of the heat stored in the heat buffer tank for sell. σ_t indicates the unit income that can be obtained by the CHP unit and the energy storage device to sell electricity to ISO. τ_t means the unit income that can be acquired by the heat buffer tank to sell heat to ISO.

D. SUPPLEMENTARY CONSTRAINTS

Constraints of power flow and power balancing of the network are also included in the proposed model, which can be seen as follows:

$$-\pi \le \theta_{\text{n,t}} \le \pi \tag{53}$$

$$-PF_{\text{n,m}} \le TB_{\text{n,m}}(\theta_{\text{n,t}} - \theta_{\text{m,t}}) \le PF_{\text{n,m}} \tag{54}$$

$$\sum_{i=1}^{NG} P_{gencoi,t} + \sum_{j=1}^{NW} P_{windj,t} + \sum_{i=1}^{NS} zd_{tsch} + \sum_{i=1}^{NCHP} P_{i,t,sch}^{\text{CHP}} = d_t \tag{55}$$

(53) describes the upper and lower phase angle limits of the node. (54) is the power flow limit of the transmission line. The power balancing constraint is given in (55).

E. MULTI-OBJECTIVE OPTIMIZATION

Considering that traditional Genco, WPP and DRA all want to maximize their interests, in order to balance the interests of all parties, this paper adopts an improved weighted method to obtain the best behavior patterns of market participants.

The objective function of the traditional weighted method is as follows:

$$\begin{aligned}OBJ = max\{&\beta_1 (GencoProfit) + \beta_2 (WPPProfit) \\ &+ \beta_3 (DRAProfit)\}\end{aligned} \tag{56}$$

where $\beta_1, \beta_2, \beta_3$ should satisfy:

$$0 \le \beta_1, \beta_2, \beta_3 \le 1 \tag{57}$$

$$\beta_1 + \beta_2 + \beta_3 = 1 \tag{58}$$

To make the weighted coefficients $\beta_1, \beta_2, \beta_3$ more comprehensive, this paper improves the traditional weighted method by combining the Analytic Hierarchy Process(AHP) and Entropy method.

The basic idea of the AHP is to first establish a hierarchical structure model by stratifying the indices according to their importance, and then construct a set of pairwise comparison matrices by comparing all the evaluation indices in each layer. The consistency test should also be done, and finally, weights are determined. Details of the AHP method can be found in [26].

The hierarchical structure model used in this paper is shown in Fig.3.

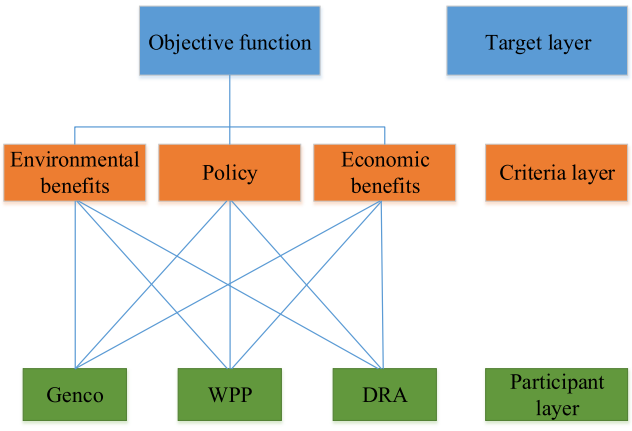

FIGURE 3. The hierarchical structure model.

As can be seen in Fig.3, the hierarchical structure model has three layers, which are the target layer, the criteria layer, and the participant layer. The weights are determined based on three indices, such as environmental benefits, policy, and economic benefits.

According to [26], we can get the weights of three participants from the point of the three indices, respectively, as can

be seen in (59-61).

$$\mathrm{A} = [a_1, a_2, a_3] \tag{59}$$
$$\mathrm{B} = [b_1, b_2, b_3] \tag{60}$$
$$\mathrm{C} = [c_1, c_2, c_3] \tag{61}$$

Actually, the weights obtained from the AHP method are subjective, reflecting the intention of decision-makers. Therefore, the Entropy method is used to evaluate the contribution of each characteristic index to the result and obtain combined objective weights based on the subjective weights.

The basic idea of the Entropy method is to determine the objective weight according to the magnitude of the index variability. The weighting step of the Entropy method is as follows: firstly, the indices are standardized, and then the information entropy of each index is obtained, and finally, the combined weights of the indices are determined.

(59-61) are used as input data for the Entropy method, and thus a standardized matrix can be derived as shown in (62).

$$\mathrm{D} = \begin{bmatrix} d_{11} & d_{12} & d_{13} \\ d_{21} & d_{22} & d_{2,3} \\ d_{31} & d_{32} & d_{33} \end{bmatrix} \tag{62}$$

In which, d_{ij} (i $= 1, 2, 3$; j $= 1, 2, 3$) denotes the weight of the participant i from the point of index j.

Equation (63) denotes the calculation of the entropy value of the index j.

$$e_j = -\frac{1}{\ln 3}\sum_{i=1}^{3}\frac{d_{ij}}{\sum_{i=1}^{3} d_{ij}} * \ln\left(\frac{d_{ij}}{\sum_{i=1}^{3} d_{ij}}\right), \quad j = 1, 2, 3 \tag{63}$$

The weight of each index can be calculated as in (64).

$$w_j = \frac{1 - e_j}{\sum_{j=1}^{3}(1 - e_j)}, \quad j = 1, 2, 3 \tag{64}$$

Finally, the proportion of each participant in the objective function can be decided in (65).

$$\beta_i = \sum\nolimits_{j=1}^{3} w_j d_{ij}, \quad i = 1, 2, 3 \tag{65}$$

The combined weight can more objectively and accurately reflect the contribution of each component to the result of the objective function, and the optimization result can reasonably reflect the market power of each participant in the market.

It is to be noted that there are many other methods to solve the multi-objective optimization problem such as heuristic algorithms, and we decide to use the improved weighted method after careful consideration. The reasons are as follows:

a. Heuristic algorithms may be stuck in local optimum, which is the major concern. However, the global optimal solution must be found by the improved weighted method proposed in this manuscript. The reason is that the multi-objective optimization problem can be transformed into a single-objective optimization problem after the weights have been determined. Then through some linearization methods, the single-objective optimization problem can be further transformed into a mixed-integer linear programming problem, and thus can be easily solved by some optimization software such as Gurobi. Thereby, we can obtain the global optimal solution. Furthermore, we combine the Analytic Hierarchy Process and Entropy method to make the weights more accurate and comprehensive.

b. The improved weighted method takes less time than heuristic algorithms. Although this manuscript focuses on the day-ahead schedule instead of the real-time schedule, which means that we have plenty of time to run our model and get the solution, we still want to indicate that according to our calculation results, the heuristic algorithm will take 8 hours and 23 minutes to get the solution while it only takes nearly 2 hours to use the improved weighted method.

Finally, it should be noted that different algorithms have their own advantages and disadvantages. So it is difficult for us to decide which one is the better one. Although this manuscript uses the improved weighted method, this does not mean that other algorithms are not good, but we think that the improved weighted method is more suitable for this manuscript.

F. LINEARIZATION

In the objective function of this paper, there exists two consecutive types of variables multiplied such as $Inc_t * Pen_t$, resulting in the non-convex of the model. To deal with the non-convex terms, this paper uses a binary expansion approach to discretize the continuous variable to a finite set of values and then uses the Big-M method to convert the product term of two integer variables to a linear term [15]. Thus the non-convex optimization problem is transformed into a convex optimization problem.

Take the term $Inc_t * Pen_t$ as an example. From (21) and (22), the range of values of Inc_t and Pen_t is known. Then the expressions of Inc_t and Pen_t can be obtained by the binary expansion approach as follows:

$$Inc_t = 0 + \frac{Inc^{max}}{MM_t} * \sum\nolimits_{n=0}^{log_2 MM_t} 2^n * k_n \tag{66}$$
$$Pen_t = 0 + \frac{Pen^{max}}{MM_t} * \sum\nolimits_{n=0}^{log_2 MM_t} 2^n * q_n \tag{67}$$

In which, k_n and q_n are binary variables. MM_t is the power function of 2 and it equals to 64 in this paper.

It can be seen from equations (66) and (67) that there exists a product term $k_n * q_n$ in the result of the term $Inc_t * Pen_t$.

Then the Big-M method is used to handle the product term $k_n * q_n$, as can be seen in (68-71).

$$\alpha_n = k_n * q_n \tag{68}$$
$$\alpha_n = q_n - r \tag{69}$$
$$k_n * 0 \le q_n - r \le k_n * 1 \tag{70}$$
$$(1 - k_n) * 0 \le r \le (1 - k_n) * 1 \tag{71}$$

In which, r is a binary variable. With the aid of (66-71), the non-convex term $Inc_t * Pen_t$ has been transformed into a linear term.

III. CASE STUDY

To obtain the optimal strategy of each market participant and validate the proposed day-ahead market model, a slightly modified version of the IEEE RTS-24 (Appendix Fig.19) is considered, which includes 32 generators (22 coal-fired unit and 10 wind turbines), loads at 17 buses, and 37 transmission lines.

Coal-fired units 1-8 are managed by Genco 1, 9-15 are managed by Genco 2, and 16-22 are managed by Genco 3. Wind turbines 1-3 are administered by WPP 1, 4-7 are operated by WPP 2, and 8-10 are managed by WPP 3. The load nodes are uniformly managed by DRA 1, and among them, nodes 1-8 each has a CHPS and an energy storage device. Wind turbines 1-7 have an installed capacity of 300 MW, and wind turbines 8-10 have an installed capacity of 500 MW. Details of the CHPS and energy storage device can be seen in the Appendix.

Using the improved weighted method, the weights of the Genco 1, 2, 3, WPP 1, 2, 3 and DRA account for 0.14, 0.08, 0.08, 0.1, 0.12, 0.18, 0.3 of the objective function respectively.

The scenario data of the wind power output is adapted from the actual data of the Irish grid in 2014-2019 [30], from which two sets of hourly wind power data are extracted.

The extraction method of the first (second) set of hourly wind power data is: Firstly, find the minimum (maximum) three days of total wind power output per month and extract hourly wind power data from these three days, thus obtaining 216 scenarios.

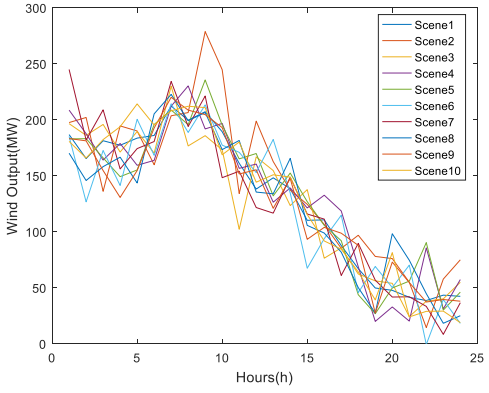

FIGURE 4. The first set of scenario data.

The two sets of data are then aggregated into ten categories separately using the K-means clustering method, and the results are shown in Fig.4 and Fig.5. Thus wind power uncertainty is taken into consideration through scenario generation.

It is considered that the wind power output of both WPP 1 and WPP 2 is consistent with the first set of scenario data because the wind turbines controlled by them are geographically close. It is also believed that the wind turbines controlled by WPP 3 are rich in wind power resources, and the wind power output of them is in line with the second set of scenario data.

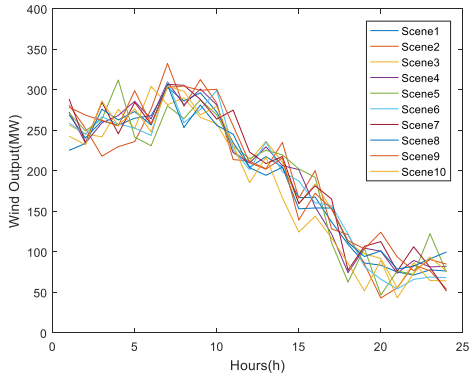

FIGURE 5. The second set of scenario data.

In this case, the unit incentive/penalty for positive/negative deviations of wind power is chosen to be 0.9/1.1 times of electricity price. The unit income that can be obtained by the CHP unit and the energy storage device to sell electricity to ISO is chosen to be 0.9 times of electricity price. The unit income that can be obtained by the heat buffer tank to sell heat to ISO is chosen to be 0.9 times of heat price. The original electricity price is set to be 15 $/MWh.

The proposed model is formulated as a mixed-integer programming (MIP) problem and solved using the GUROBI solver in Yalmip.

The TOU optimization results are shown in Table 1.

TABLE 1. TOU optimization results.

	Valley	Off-peak	Peak
Time period(h)	1-7&&23-24	8-17	18-22
Electricity price($/MWh)	8.5	15	28.3

This paper does not consider the thermal network and the source thermal power plant, and since consumers have little market power in the thermal market, consumers are regarded as the recipient of the thermal price. The thermal price is shown in Table 2.

TABLE 2. Thermal price.

	Valley	Off-peak	Peak
Time period(h)	1-4	8-18	5-8&&19-24
Thermal price($/MWth)	7	12	25

Fig.6 compares the load consumption before and after the implementation of the DRP. The blue/red line represents the load curve before/after the implementation of the DRP. It can be seen that the load consumption curve has become smoother, and the peak-to-valley difference has been reduced significantly, which shows the necessity and superiority of implementing DRP.

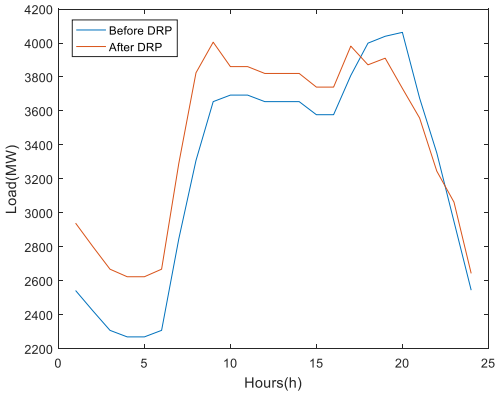

FIGURE 6. Comparison of the load consumption before and after the implementation of the DRP.

To investigate the impact of CHPS and energy storage devices on the behavior patterns of market participants, four situations are considered as follows:

Situation 1: With no CHPS and energy storage device.

Situation 2: Only include CHPS.

Situation 3: Only include the energy storage device.

Situation 4: Include CHPS and energy storage devices simultaneously.

It is to be noted that general parameters such as network topology, load value, and generator data are consistent in these four situations.

The four situations will then be compared and discussed from five perspectives of WPP output, Genco output, Energy storage device operation, CHPS operation, and DRA profit.

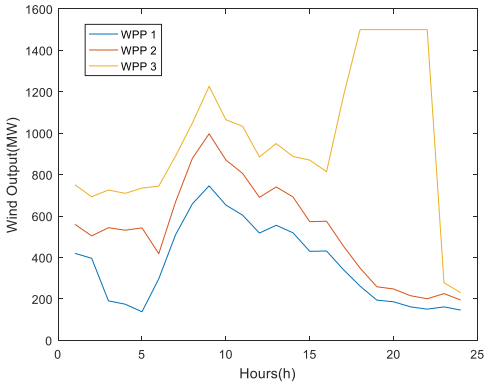

FIGURE 7. Wind output curves of WPPs in situation 4.

1) WPP

Wind output curves of WPPs in situation 4 is shown in Fig.7. It can be seen from Fig.7 that the output curves of WPP 1 and 2 are similar, and the output curve of WPP 2 is slightly higher than 1, this is because WPP 2 owns four wind turbines whereas WPP 1 only has three wind turbines.

In common with WPP 1, WPP 3 owns three wind turbines; however, WPP 3's 24-hour output plan is much larger than WPP 1 or 2. This is mainly because the wind turbines controlled by WPP 1 and WPP 2 are located close to each other, and their wind power resource endowments are relatively close; while WPP 3 is located at a location where wind power is relatively abundant. This shows that the location of the wind turbine has a significant impact on its participation in the market and the submission of the output plan.

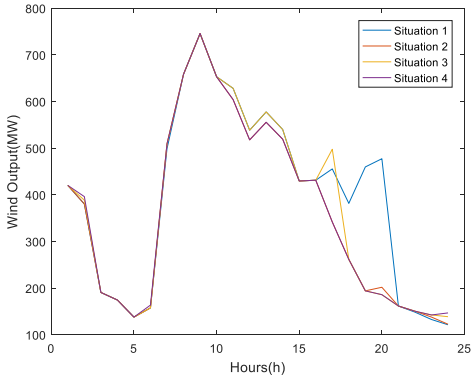

FIGURE 8. Comparison of WPP 1 output plans for the four situations.

Fig.8 shows the comparison of WPP 1 output plans for the four situations. Analysis of Fig.8 reveals two phenomena:

(1) During 0-16h, the output curves of WPP 1 in the four situations almost coincide, and the wind power output under situation 2 and situation 4 is slightly lower than the other two situations during 11-16 h.

(2) During 18-22h, the output of WPP 1 in situation 1 is greater than the output of the other three situations.

The cause of phenomenon 1 is that the energy storage devices in situation 3 and situation 4 do not supply power to the load during 0-16h, but purchase cheap electricity from ISO for hoarding to sell at the peak of the electricity price, so the energy storage devices in these two situations have no effect on the wind power output plan. The CHP units in situation 2 and situation 4 will supply the load during 11-16h, causing the load to reduce the power demand of conventional generators and wind turbines, which results in the wind power output curve in situations 2 and 4 during 11-16h slightly lower than the other two situations.

For situation 2, although the CHP unit continues to supply power to the load during 0-10h when wind power resource is rich, the traditional Genco will reduce the output appropriately and the WPP will not be affected because WPP in the total objective function accounts for a higher proportion than Genco; for situation 4, the CHP unit's electricity output is all supplied to the energy storage device for hoarding during 0-10h, so there will be no impact on the wind power output plan.

The cause of phenomenon 2 is: during 0-16h, the electricity price is in the valley or off-peak period, and the energy storage devices in situations 3 and 4 will purchase electricity from ISO during this time. The energy storage device will provide some power to the load and sell the electricity to ISO for profit during peak hours, which will result in a reduction in the total amount of load to be powered by conventional generators

and wind turbines, thus the wind power output plans for situation 3 and 4 during 18-22 hours are lower compared to situation 1. Although there is no energy storage device in situation 2, the CHP unit will shoulder the responsibility of supplying partial power to the load, which will also reduce the total load that is left to be powered by conventional generators and wind power plants, resulting in a decline in wind power output plans.

2) GENCO

Fig.9 shows the comparison of planned output of each traditional Genco under situation 4.

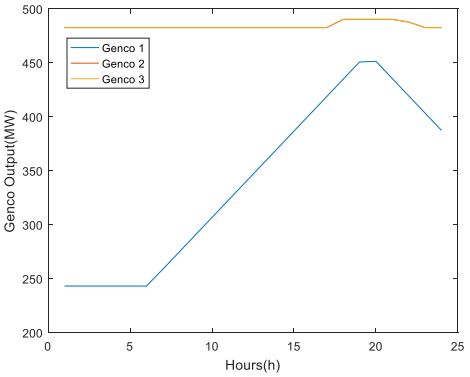

FIGURE 9. Comparison of planned output of each traditional Genco under situation 4.

It can be seen from Fig.9 that the output curves of Genco 2 and 3 coincide and remain almost constant, whereas the planned output curve of Genco 1 has a steep climb process around 6-10 pm.

The main reason for this phenomenon is that the generators controlled by Genco 1 are all located in the I area, the generators controlled by Genco 2 and 3 are located in the II area, and 7 out of 10 wind turbines are located in the I area. During 18-22h, wind power resources are scarce, and the load demand is very high. To maintain the load balance in Area I, Genco 1 has to increase its output significantly, thus causing its planned output curve to undergo a steep climb process.

Fig.10 shows the comparison of the output plans of Genco 1 in the four situations.

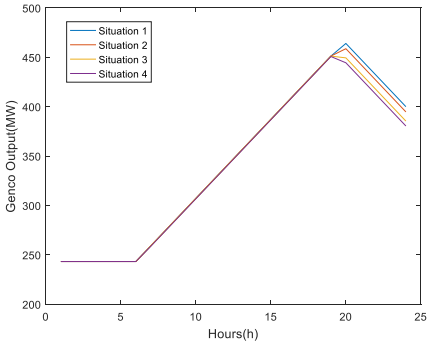

FIGURE 10. Comparison of the output plans of Genco 1 in the four situations.

It can be seen from Fig.10 that the output plan curves of Genco 1 during 0-17h are basically coincident under the four situations. There are some differences during 18-22h, in which situation 1 has the highest output curve, situation 2 ranks second, and situation 4 has the lowest output curve.

The reason for the difference among output curves during 18-22h is that this period is the peak period of the demand curve, and load will be partially supplied by CHP units and energy storage device in situation 4, which will result in the phenomenon that the Genco output curve in situation 4 is lower than the other three situations. The CHP unit in situation 2 can provide less electricity than the energy storage device in situation 3 during the peak load period, so the Genco output curve for situation 2 will be higher than situation 3.

3) ENERGY STORAGE DEVICE

As to the energy storage device, Fig.11 shows a comparison of the operation of buying and selling electricity in situations 3 and 4.

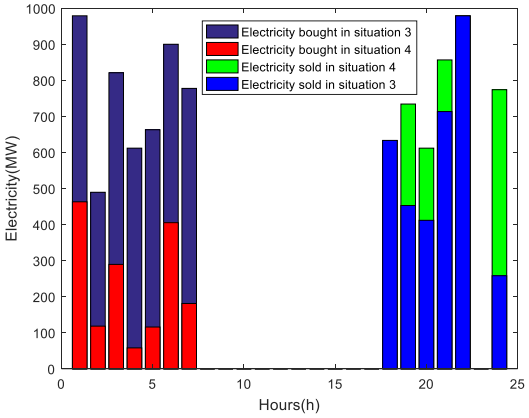

FIGURE 11. Comparison of the operation of buying and selling electricity in situation 3 and 4.

It can be seen from Fig.11 that the energy storage devices in situation 3 and 4 will purchase electricity from ISO during the valley period (0-7h) for storage, and sell the electricity during the peak period of electricity price (18-22h) to increase the load-side revenue. Due to the limitation of the discharge rate of the energy storage device, it is impossible to sell all the electricity before 10 pm so that the remaining electricity will be sold out at midnight.

During 0-7h, the energy storage device in situation 3 buys more electricity than situation 4. This is because situation 4 has CHP units, and the CHP units can provide energy for the energy storage device, which reduces the quantity of electricity to be bought. It can be seen from Fig.11 that the energy storage device of situation 4 sells more electricity than that of situation 3 during 18-22h, which is also due to the existence of the CHP unit.

4) CHPS

The power output and heat output values of the CHP unit in situation 2 and situation 4 are identical, as shown in Fig.12 and Fig.13.

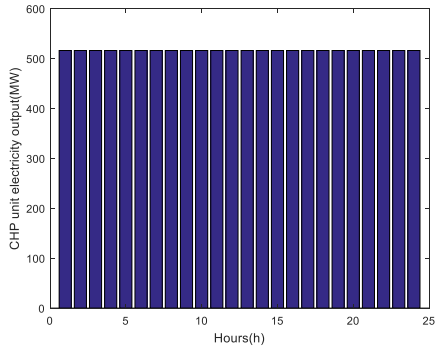

FIGURE 12. The power output values of the CHP unit in situation 2 and situation 4.

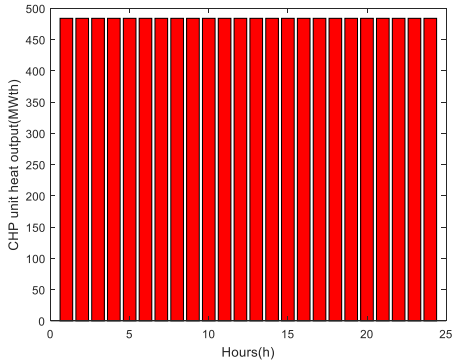

FIGURE 13. The heat output values of the CHP unit in situation 2 and situation 4.

As can be seen from Fig.12 and Fig.13, the CHP units remain operational for 24 hours and the output remains constant. However, the electricity output of the CHP unit in situation 4 is not wholly used for load supply or sold to ISO, and a considerable part is transmitted to the energy storage device for hoarding, so as to sell it during the peak period of electricity price for profit. The distribution structures of the output power of the CHP unit in situations 4 and 2 are shown in Fig.14 and Fig.15, respectively.

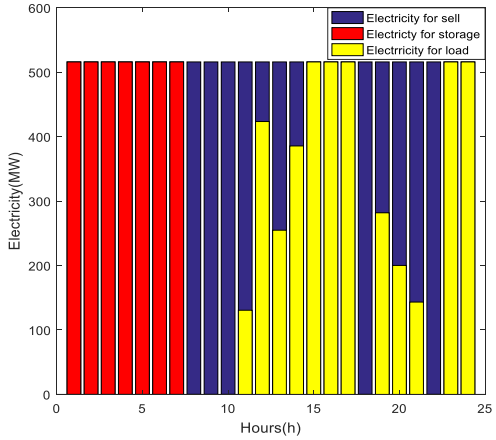

FIGURE 14. Distribution structure of the output power of the CHP unit in situation 4.

The red color in Fig.14 and Fig.15 represents the portion of the CHP unit power output that transmitted to the energy

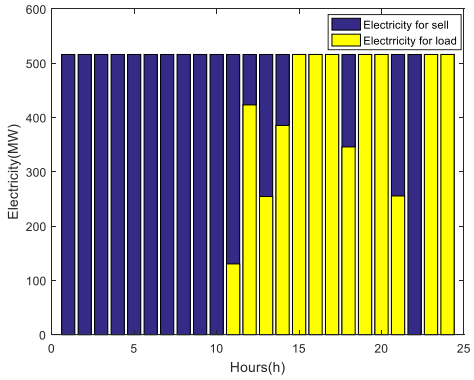

FIGURE 15. Distribution structure of the output power of the CHP unit in situation 2.

storage device. Blue represents the portion sold to ISO, and yellow represents the portion provided for the load.

Comparing Fig.14 and Fig.15, it can be found that since situation 4 has an energy storage device and situation 2 does not, the output power of the CHP unit during 0-7h in Fig.14 has all been transmitted to the energy storage device for storage in order to sell at peak price later, whereas the entire energy has to be sold to ISO in Fig.15, resulting in a reduction in profit compared to Fig.14.

It can also be found that during 18-20h, the CHP unit will sell most of its electricity output to ISO in Fig.14, whereas in Fig.15, most of the CHP unit's electricity output is provided for the load. The main reason for the difference is that situation 4 has an energy storage device that can supply electricity to the load, so the CHP unit will tend to sell electricity; whereas situation 2 has no energy storage device, and as a result, the CHP unit will tend to provide power for the load during peak electricity price period.

Since the heat output from the CHP unit and the boiler unit is all supplied to the heat buffer tank, only the heat change in the heat buffer tank is studied in this paper. In fact, in the model proposed in this paper, only the heat buffer tank can participate in the thermal market for heat trading, so the operation of buying and selling heat in situation 2 and situation 4 should be consistent, as shown in Fig.16.

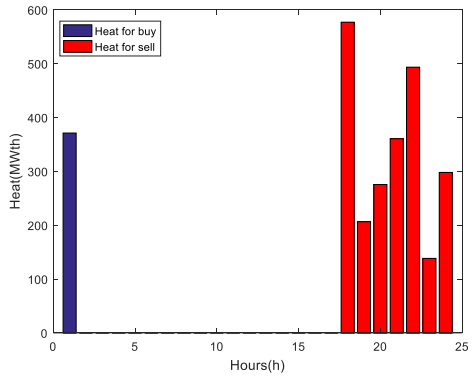

FIGURE 16. The operation of buying and selling heat in situation 2 and situation 4.

As can be seen from Fig.16, the heat buffer tank purchases heat at 1 am to store, and sells the heat at the peak period of the heat demand to make a profit, i.e.18-24h.

5) DRA PROFIT

The profit values of the DRA in the four situations in compared in Table 3:

TABLE 3. Comparison of the profit values of the DRA in the four situations.

Situation	1	2	3	4
DRA Profit($)	208486	247461	220525	260669

As can be seen from Table 3, situation 1 has the least profit, situation 4 has the most profit, and situation 2 has a profit greater than situation 3.

Subtracting the profit of situation 1 from the profit of situation 2 can obtain the profit growth of the CHPS to the DRA, which is 38975$, and subtracting the profit of situation 1 from the profit of situation 3 can achieve the profit growth of energy storage device to the DRA, which is 12039$. The profit of situation 4 minus the profit of situation 1 equals the profit growth of the CHPS and the energy storage device to the DRA, which is 52183$.

Considering CHPS independently is more profitable for the DRA than considering the energy storage device alone. This is because that the CHPS can participate in both the electricity market and the thermal market, whereas the energy storage device can only participate in the electricity market.

Considering the CHPS and the energy storage device simultaneously can bring more growth of profit to the DRA than the sum of their individual effects. It is because that considering both the CHP unit and the energy storage device enables the interaction between them, for example, the CHP unit can transmit part of its electricity output to the storage device for hoarding and sell it during peak price period to make a profit.

It should be noted that load profiles may vary in different days which will influence the results, but the volatility of load profiles are not considered in this paper. The reason is that compared to wind power, the load profile is less uncertain and volatile, and it can be predicted by modern technology accurately. Thus only the uncertainty of wind power is considered and the load profile of a particular day is used in the case study.

6) IMPACT OF PARTICIPATION COEFFICIENTS θ

In equation (20), the penalty value will change as the contract value $d_t^{Contract}$ changes, which in turn will cause the DRA profit to change.

Similarly, the DRA profit will be influenced by the dissatisfaction function value c in equation (23).

Analyses have been carried out to understand the impact of contract value $d_t^{Contract}$ and participation coefficients θ on the profit values of the DRA in situation 4.

Fig.17 shows the variation of DRA profit with variations in the parameter θ over the range from 0 to 1 (for fixed values of other parameters). It is noted that as θ increases, there is an increase in the DRA profit.

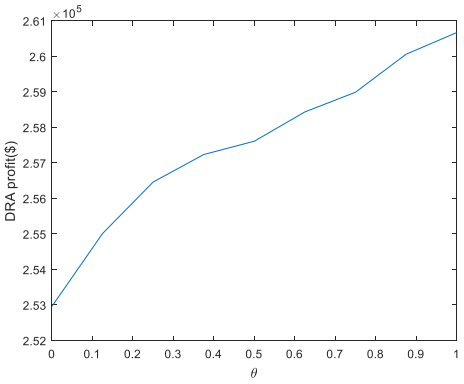

FIGURE 17. DR profits with variation in θ.

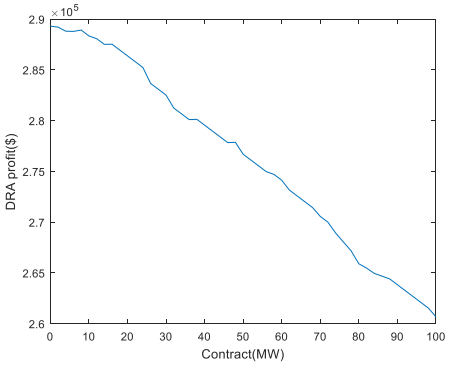

FIGURE 18. DR profits with variation in the contract value.

Fig.18 shows the variation of DRA profit with variations in the parameter $d_t^{Contract}$ over the range from 0 to 100 MW (for fixed values of other parameters). It can be seen from Fig.18 that as the contract value increases, there is a decrease in the DRA profit.

IV. CONCLUSION

This paper proposes a multi-participant day-ahead energy market schedule model that takes into account demand response programs. Wind power producers (WPP) are modeled in this paper and there is no difference between WPP and traditional generators in clearing the market. DRA that includes both CHPS and energy storage devices is modeled. In addition to participating in the electricity market, DRA can also participate in the thermal market by buying and selling heat stored in the heat buffer tank. This paper comprehensively considers the objective function of multiple market participants and uses the improved weighted method to solve the multi-objective optimization problem. Considering the uncertainty of wind power, the K-means clustering method is used to generate multiple representative wind power output scenarios.

Through the analysis of the IEEE RTS-24 test system, the optimal day-ahead schedule strategy for each market participant is obtained. It can be seen from the calculation results of the case that by implementing the DRPs, the demand

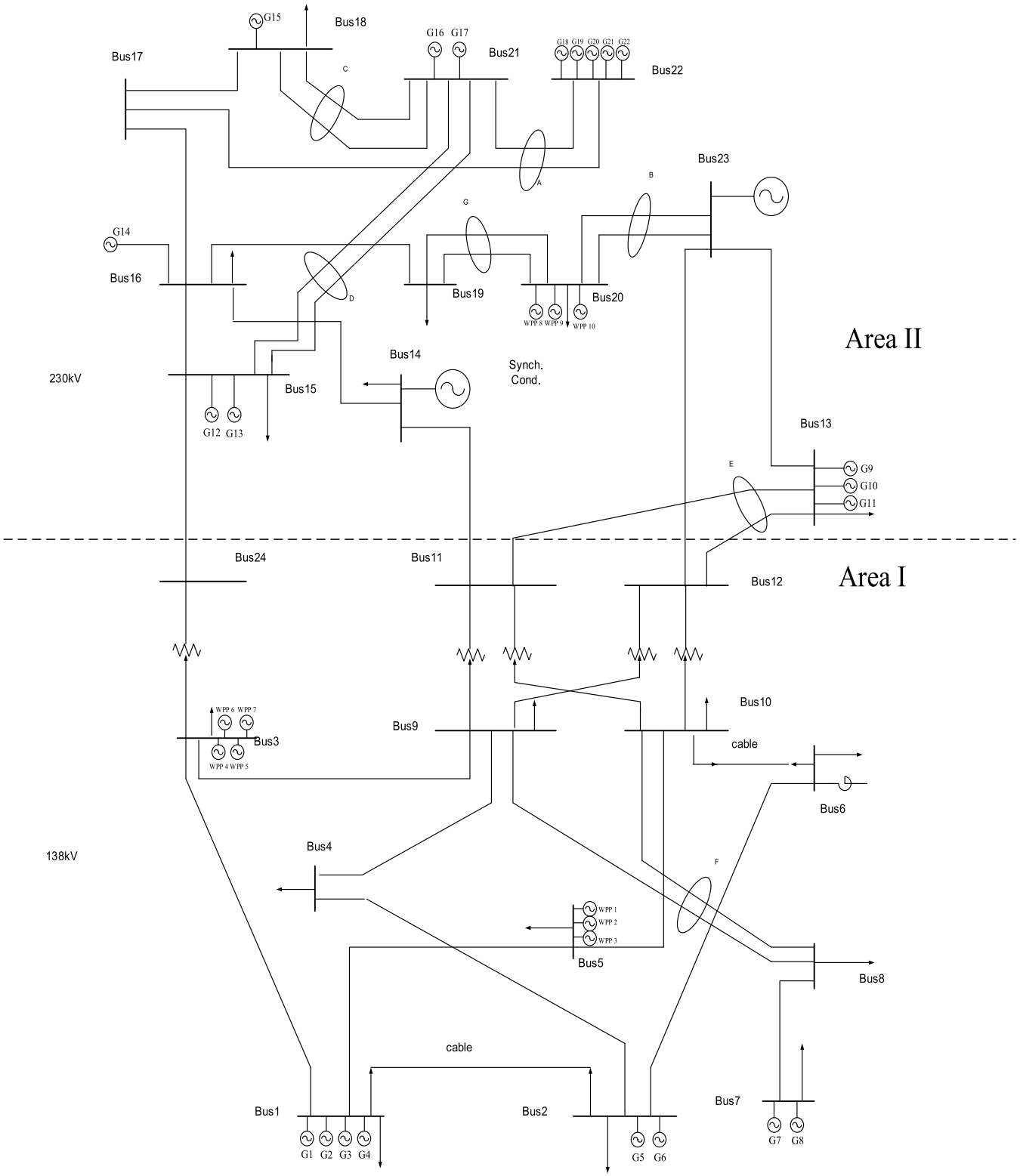

FIGURE 19. The diagram of the modified IEEE RTS-24 test system.

curve becomes smoother, and the peak-to-valley difference is significantly reduced. Due to the volatility of wind power output, traditional Gencos are still the mainstay of power generation when wind power resources are scarce or demand curve reaches its peak period. The energy storage device and the heat buffer tank will purchase a large amount of power for storage when the electricity price (heat price) is at the bottom, and the electricity (heat) can be sold during the peak period of the electricity (heat) price. Owing to the high efficiency and economic benefits, the CHP unit remains operational

for 24 hours. Considering the CHPS and the energy storage device simultaneously can bring more growth of profit to the DRA than the sum of their individual effects due to the interaction between them.

Future work includes:

1) Analyze the power usage behavior of the load and enhance the accuracy of the demand response modeling;
2) Study strategies for market participants in the reserve and capacity markets.

APPENDIX

See Figs. 19 and 20 and Tables 4 and 5.

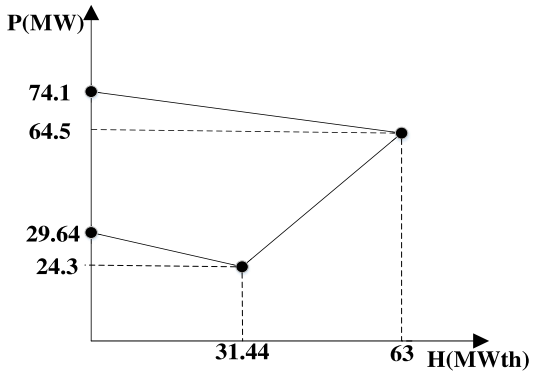

FIGURE 20. The FOR of a single CHP unit.

TABLE 4. Data of the heat buffer tank.

β_{gain}	β_{loss}	η	B_{max}^{charge}	$B_{max}^{discharge}$	B_{max}	B_{min}
0.3	0.6	1	65	65	600	0
MWth	MWth	%	MWth/h	MWth/h	MWth	

TABLE 5. Data of the energy storage device.

η^{char}	η^{dis}	M^{char}	M^{dis}	S^{max}	S^{min}
0.9	0.9	122.4	122.4	700	0
		MW/h	MW/h	MW	

REFERENCES

[1] *Energy Policy Act of 2005 (Section 1252, Feb 2006)*, U.S. Dept. Energy, Washington, DC, USA, 2005.

[2] M. Parvania, M. Fotuhi-Firuzabad, and M. Shahidehpour, "Optimal demand response aggregation in wholesale electricity markets," *IEEE Trans. Smart Grid*, vol. 4, no. 4, pp. 1957–1965, Dec. 2013, doi: 10.1109/TSG.2013.2257894.

[3] N. Mahmoudi, E. Heydarian-Forushani, M. Shafie-khah, T. K. Saha, M. Golshan, and P. Siano, "A bottom-up approach for demand response aggregators' participation in electricity markets," *Electr. Power Syst. Res.*, vol. 143, pp. 121–129, Feb. 2017.

[4] R. Henríquez, G. Wenzel, D. E. Olivares, and M. Negrete-Pincetic, "Participation of demand response aggregators in electricity markets: Optimal portfolio management," *IEEE Trans. Smart Grid*, vol. 9, no. 5, pp. 4861–4871, Sep. 2018.

[5] M. Vahid-Ghavidel, M. Nadali, and M.-I. Behnam, "Self-scheduling of demand response aggregators in short-term markets based on information gap decision theory," *IEEE Trans. Smart Grid*, vol. 10, no. 2, pp. 2115–2126, Mar. 2018.

[6] H. M. Soliman and A. Leon-Garcia, "Game-theoretic demand-side management with storage devices for the future smart grid," *IEEE Trans. Smart Grid*, vol. 5, no. 3, pp. 1475–1485, May 2014.

[7] M. Motalleb, A. Annaswamy, and R. Ghorbani, "A real-time demand response market through a repeated incomplete-information game," *Energy*, vol. 143, pp. 424–438, Jan. 2018.

[8] M. Motalleb, P. Siano, and R. Ghorbani, "Networked stackelberg competition in a demand response market," *Appl. Energy*, vol. 239, pp. 680–691, Apr. 2019, doi: 10.1016/j.apenergy.2019.01.174.

[9] W. Xie, P. Zhang, R. Chen, and Z. Zhou, "A nonparametric Bayesian framework for short-term wind power probabilistic forecast," *IEEE Trans. Power Syst.*, vol. 34, no. 1, pp. 371–379, Jan. 2019.

[10] M. Cui, V. Krishnan, B.-M. Hodge, and J. Zhang, "A copula-based conditional probabilistic forecast model for wind power ramps," *IEEE Trans. Smart Grid*, vol. 10, no. 4, pp. 3870–3882, Jul. 2019.

[11] L. Exizidi, J. Kazempour, and A. Papakonstantinou, "Incentive-compatibility in a two-stage stochastic electricity market with high wind power penetration," *IEEE Trans. Power Syst.*, vol. 34, no. 4, pp. 2846–2858, Jul. 2019, doi: 10.1109/TPWRS.2019.2901249.

[12] C. E. L. Hiroux and M. Saguan, "Large-scale wind power in European electricity markets: Time for revisiting support schemes and market designs?" *Energy Policy*, vol. 38, no. 7, pp. 3135–3145, Jul. 2010.

[13] J. M. Morales, A. J. Conejo, and J. Pérez-Ruiz, "Short-term trading for a wind power producer," *IEEE Trans. Power Syst.*, vol. 25, no. 1, pp. 554–564, Feb. 2010.

[14] R. A. Jabr and B. C. Pal, "Intermittent wind generation in optimal power flow dispatching," *IET Gener., Transmiss. Distrib.*, vol. 3, no. 1, pp. 66–74, Jan. 2009.

[15] M. Asensio and J. Contreras, "Risk-constrained optimal bidding strategy for pairing of wind and demand response resources," *IEEE Trans. Smart Grid*, vol. 8, no. 1, pp. 200–208, Jan. 2017.

[16] J. Aabakken, *Power Technologies Energy Data Book*. Golden, CO, USA: National Renewable Energy Lab, 2006.

[17] Z. W. Geem and Y. Cho, "Handling non-convex heat-power feasible region in combined heat and power economic dispatch," *Int. J. Electr. Power Energy Syst.*, vol. 34, no. 1, pp. 171–173, Jan. 2012, doi: 10.1016/j.ijepes.2011.08.024.

[18] M. Alipour, B. Mohammadi-Ivatloo, and K. Zare, "Stochastic risk-constrained short-term scheduling of industrial cogeneration systems in the presence of demand response programs," *Appl. Energy*, vol. 136, pp. 393–404, Dec. 2014.

[19] M. Alipour, B. Mohammadi-Ivatloo, and K. Zare, "Stochastic scheduling of renewable and CHP-based microgrids," *IEEE Trans. Ind. Informat.*, vol. 11, no. 5, pp. 1049–1058, Oct. 2015.

[20] M. Alipour, K. Zare, H. Seyedi, and M. Jalali, "Real-time price-based demand response model for combined heat and power systems," *Energy*, vol. 168, pp. 1119–1127, Feb. 2019.

[21] M. Alipour, K. Zare, and B. Mohammadi-Ivatloo, "Short-term scheduling of combined heat and power generation units in the presence of demand response programs," *Energy*, vol. 71, pp. 289–301, Jul. 2014, doi: 10.1016/j.energy.2014.04.059.

[22] M. Alipour, K. Zare, and H. Seyedi, "A multi-follower bilevel stochastic programming approach for energy management of combined heat and power micro-grids," *Energy*, vol. 149, pp. 135–146, Apr. 2018, doi: 10.1016/j.energy.2018.02.013.

[23] Y. Chen, W. Wei, F. Liu, E. E. Sauma, and S. Mei, "Energy trading and market equilibrium in integrated heat-power distribution systems," *IEEE Trans. Smart Grid*, vol. 10, no. 4, pp. 4080–4094, Jul. 2019.

[24] L. Deng, Z. Li, H. Sun, Q. Guo, Y. Xu, R. Chen, J. Wang, and Y. Guo, "Generalized locational marginal pricing in a heat-and-electricity-integrated market," *IEEE Trans. Smart Grid*, vol. 10, no. 6, pp. 6414–6425, Nov. 2019.

[25] Y. Cao, W. Wei, L. Wu, S. Mei, M. Shahidehpour, and Z. Li, "Decentralized operation of interdependent power distribution network and district heating network: A market-driven approach," *IEEE Trans. Smart Grid*, vol. 10, no. 5, pp. 5374–5385, Nov. 2018.

[26] I. Basak and T. Saaty, "Group decision making using the analytic hierarchy process," *Math. Comput. Model.*, vol. 17, no. 4, pp. 101–109, Feb./Mar. 1993.

[27] M. Shafie-Khah and J. P. Catalão, "A stochastic multi-layer agent-based model to study electricity market participants behavior," *IEEE Trans. Power Syst.*, vol. 30, no. 2, pp. 867–881, Mar. 2014.

[28] N. I. Nwulu and X. Xia, "Multi-objective dynamic economic emission dispatch of electric power generation integrated with game theory based demand response programs," *Energy Convers. Manage.*, vol. 89, pp. 963–974, Jan. 2015.

[29] H. A. Aalami, M. P. Moghaddam, and G. R. Yousefi, "Demand response modeling considering interruptible/curtailable loads and capacity market programs," *Appl. Energy*, vol. 87, no. 1, pp. 243–250, 2010.

[30] *System and Renewable Data*. Accessed: Jun. 30, 2019. [Online]. Available: http://www.eirgridgroup.com

CHUNYAN LI was born in 1975. She received the B.S., M.S., and Ph.D. degrees in electrical engineering from Chongqing University, in 1998, 2001, and 2008, respectively. She had been a Visiting Scholar with Tulsa University, USA. During this visit, she collaborated with Professor H. M. Tai of Tulsa University on the smart grid and distributed generation. In 2003, she joined Chongqing University, where she has been an Associate Professor with the Department of Electrical Engineering, since 2008. From October 2013 to October 2014, she was a Visiting Scholar with the Texas University of Agriculture and Technology. She presided over or participated in more than 30 scientific research projects. She has published more than 40 articles. Her current research fields are power system analysis, renewable energy consumption, and smart grid dispatching.

YIMING YAO was born in 1997. He received the B.S. degree in electrical engineering from Chongqing University, Chongqing, China, in 2019, where he is currently pursuing the master's degree with the Department of Electrical Engineering. His current research interests include demand response and power system flexibility.

CHENYU ZHAO was born in 1995. She received the B.S. degree in electrical engineering from the University of Electronic Science and Technology of China, Chengdu, China, in 2017. She is currently pursuing the M.S. degree with the Department of Electrical Engineering, Chongqing University. Her current research interests include demand response and power system analysis.

XIN WANG was born in 1996. He received the B.S. degree in electrical engineering from Nanchang University, Jiangxi, China, in 2018. He is currently pursuing the M.S. degree with the Department of Electrical Engineering, Chongqing University. His current research interests include demand response and energy storage system.